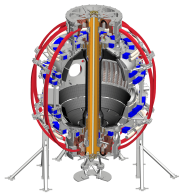




Initial applications of the non-Maxwellian extension of the full-wave TORIC v.5 code in the mid/high harmonic and minority heating regimes

Nicola Bertelli, E. Valeo, and C. K. Phillips
PPPL

57th APS-DPP Conference, Savannah, GA, November 16-20, 2015



- Full wave code TORIC
 - Brief code description
 - TORIC's versions
- Non-Maxwellian extension of TORIC v.5 in minority heating regime
 - Test I: Numerical vs. analytical Maxwellian case in TORIC
 - Bi-Maxwellian distribution
- Non-Maxwellian extension of TORIC v.5 in HHFW heating regime
 - Test I: Numerical vs. analytical Maxwellian full hot dielectric tensor
 - Test II: Numerical vs. analytical Maxwellian case in TORIC
 - Bi-Maxwellian distribution
 - Slowing-down distribution
- Conclusions

- The TORIC code solves the wave equation

$$\nabla \times \nabla \times \mathbf{E} = \frac{\omega^2}{c^2} \left[\mathbf{E} + \frac{4\pi i}{\omega} (\mathbf{J}^P + \mathbf{J}^A) \right]$$

for the electric field \mathbf{E} .

- \mathbf{J}^A → prescribed antenna current density
- \mathbf{J}^P → plasma current density

$$\mathbf{J}^P(\mathbf{x}) = \int d\mathbf{x}' \boldsymbol{\sigma}(\mathbf{x}, \mathbf{x}') \cdot \mathbf{E}(\mathbf{x}')$$

- Conductivity tensor $\boldsymbol{\sigma}[f_0(\mathbf{x}, \mathbf{v})]$, is a functional of f_0 , which is, in general, non-Maxwellian
- Spectral ansatz

$$\mathbf{E}(\mathbf{r}, t) = \sum_{m,n} \mathbf{E}^{mn}(\psi) e^{i(m\theta + n\phi - \omega t)}$$

m → poloidal mode number; n → toroidal mode number

- Principal author M. Brambilla (IPP Garching, Germany)

TORIC code (2)

- For each toroidal component one has to solve a (formally infinite) system of coupled ordinary differential equations for the physical components of $E^{mn}(\psi)$, written in the local field-aligned orthogonal basis vectors.
- The Spectral Ansatz transforms the θ -integral of the constitutive relation into a convolution over poloidal modes.
- Due to the toroidal axisymmetry, the wave equations are solved separately for each toroidal Fourier component.
- A spectral decomposition defines an accurate representation of the "local" parallel wave-vector
$$k_{\parallel}^m = (m\nabla\theta + n\nabla\phi) \cdot \hat{\mathbf{b}}$$
- The ψ variation is represented by Hermite cubic finite elements

TORIC's versions

- TORIC: IC frequency regime
extended to include non-Maxwellian ions to the second order in $k_{\perp} v_{\perp} / \Omega_c$
(part of the initial work shown by E. J. Valeo at APS-DPP 2011):
ADDITIONAL TESTS & INITIAL APPLICATIONS in THIS WORK
- TORIC-HHFW: High Harmonic Fast Wave regime
to extend to include non-Maxwellian ions: THIS WORK
- TORIC-LH: LH frequency regime
extended to include non-Maxwellian electrons
J. C. Wright *et al*, Nucl. Fusion **45** (2005) 1411 &
J. C. Wright *et al*, Commun. Comput. Phys. **4** (2008) 545

Non-Maxwellian extension of TORIC v.5 in minority heating regime

FLR non-Maxwellian susceptibility in a local coordinate (Stix) frame
 $(\hat{x}, \hat{y}, \hat{z})$, with $\hat{z} = \hat{\mathbf{b}}$, $\mathbf{k} \cdot \hat{\mathbf{y}} = 0$, to second order in $k_{\perp} v_{\perp} / \omega_c$

$$\begin{aligned}
 \chi_{xx} &= \frac{\omega_{\text{p},s}^2}{\omega} \left[\frac{1}{2} (A_{1,0} + A_{-1,0}) - \frac{\lambda}{2} (A_{1,1} + A_{-1,1}) + \frac{\lambda}{2} (A_{2,1} + A_{-2,1}) \right] \\
 \chi_{xy} &= -\chi_{yx} = i \frac{\omega_{\text{p},s}^2}{\omega} \left[\frac{1}{2} (A_{1,0} - A_{-1,0}) - \lambda (A_{1,1} - A_{-1,1}) + \frac{\lambda}{2} (A_{2,1} - A_{-2,1}) \right] \\
 \chi_{xz} &= +\chi_{zx} = -\chi_{yx} = \frac{\omega_{\text{p},s}^2}{\omega} \left(\frac{1}{2} \frac{k_{\perp}}{\omega} \right) \left[(B_{1,0} + B_{-1,0}) - \lambda (B_{1,1} + B_{-1,1}) + \frac{\lambda}{2} (B_{2,1} + B_{-2,1}) \right] \\
 \chi_{yy} &= \frac{\omega_{\text{p},s}^2}{\omega} \left[2\lambda A_{0,1} + \frac{1}{2} (A_{1,0} + A_{-1,0}) - \frac{3\lambda}{2} (A_{1,1} + A_{-1,1}) + \frac{\lambda}{2} (A_{2,1} + A_{-2,1}) \right] \\
 \chi_{yz} &= -\chi_{zy} = i \frac{\omega_{\text{p},s}^2}{\omega} \left(\frac{k_{\perp}}{\omega} \right) \left[B_{0,0} - \lambda B_{0,1} - \frac{1}{2} (B_{1,0} + B_{-1,0}) - \lambda (B_{1,1} + B_{-1,1}) \right. \\
 &\quad \left. - \frac{\lambda}{4} (B_{2,1} + B_{-2,1}) \right] \\
 \chi_{zz} &= \frac{2\omega_{\text{p}}^2}{k_{\parallel} w_{\perp}^2} \left[(1 - \lambda) B_{0,0} + \int_{-\infty}^{+\infty} dv_{\parallel} \int_0^{+\infty} dv_{\perp} v_{\perp} \frac{v_{\parallel}}{\omega} f_0(v_{\parallel}, v_{\perp}) \right] \\
 &\quad + \frac{\lambda}{2} \frac{\omega_{\text{p}}^2}{\omega} \left[2 \frac{\omega - \omega_c}{k_{\parallel} w_{\perp}^2} B_{1,0} + 2 \frac{\omega + \omega_c}{k_{\parallel} w_{\perp}^2} B_{-1,0} \right] \qquad \lambda \equiv \frac{1}{2} \left(\frac{k_{\perp} v_{\perp}}{\omega_c} \right)^2
 \end{aligned}$$

Beyond Maxwellian (2)

Evaluations of the FLR susceptibility requires computation of two functions $A_{n,j}$ $B_{n,j}$, for $n = -2 \dots 2$, $j = 0, 1$, which are v_{\perp} moments of resonant integrals of $f_0(\psi, \frac{B}{B_{\min}}, v_{\parallel}, v_{\perp})$

$$\left\{ \begin{array}{c} A_{n,j} \\ B_{n,j} \end{array} \right\} = \int_{-\infty}^{\infty} dv_{\parallel} \left\{ \begin{array}{c} 1 \\ v_{\parallel} \end{array} \right\} \frac{1}{\omega - k_{\parallel} v_{\parallel} - n\omega_c} \int_0^{+\infty} 2\pi v_{\perp} dv_{\perp} H_j(v_{\parallel}, v_{\perp})$$

with

$$H_0(v_{\parallel}, v_{\perp}) = \frac{1}{2} \frac{k_{\parallel} w_{\perp}^2}{\omega} \frac{\partial f_0}{\partial v_{\parallel}} - \left(1 - \frac{k_{\parallel} v_{\parallel}}{\omega}\right) f_0(v_{\parallel}, v_{\perp})$$

$$H_1(v_{\parallel}, v_{\perp}) = \frac{1}{2} \frac{k_{\parallel} w_{\perp}^2}{\omega} \frac{\partial f_0}{\partial v_{\parallel}} \frac{v_{\perp}^4}{w_{\perp}^4} - \left(1 - \frac{k_{\parallel} v_{\parallel}}{\omega}\right) f_0(v_{\parallel}, v_{\perp}) \frac{v_{\perp}^2}{w_{\perp}^2}$$

and

$$w_{\perp}^2 \equiv \int_{-\infty}^{\infty} dv_{\parallel} \int_0^{+\infty} 2\pi v_{\perp} dv_{\perp}^2 f_0(v_{\parallel}, v_{\perp})$$

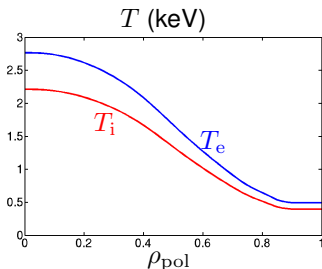
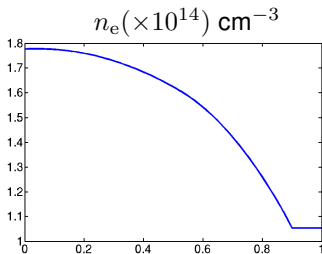
χ is pre-computed to reduce TORIC-IC runtime

- A set of N_ψ files is constructed, each containing the principal values and residues of χ for a single species on a uniform (v_\parallel, θ) mesh, for a specified flux surface ψ_j
- The distribution, $f(v_\parallel, v_\perp)$, is specified in functional form at the minimum field strength point $B(\theta) = B_{\min}$ on ψ_j
- An interpolator returns the components of χ or ε (i.e., the dielectric tensor).

Alcator C-Mod case

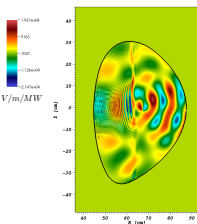
Main parameters:

- Plasma species: electron, D, and minority H (4%)
- $B_T = 5 \text{ T}$
- $I_p = 1047 \text{ kA}$
- $q(0) = 0.885$
- q at plasma edge = 4.439
- $T_e(0) = 2.764 \text{ keV}$
- $n_e(0) = 1.778 \times 10^{14} \text{ cm}^{-3}$
- $T_{D,H}(0) = 2.212 \text{ keV}$
- TORIC resolution:
 $n_{\text{mod}} = 255, n_{\text{elm}} = 480$

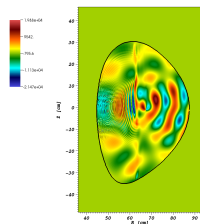


Excellent agreement between numerical and analytical evaluation of the electric field and in terms of absorbed power

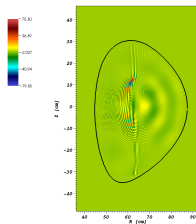
Maxw. analytical: $\text{Re}(E_-)$



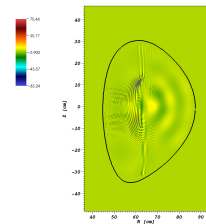
Maxw. numerical: $\text{Re}(E_-)$



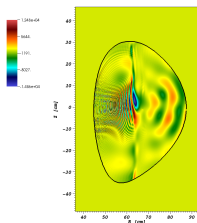
Maxw. analytical: $\text{Re}(E_{||})$



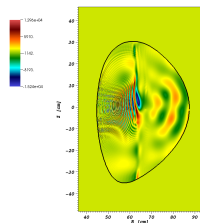
Maxw. numerical: $\text{Re}(E_{||})$



Maxw. analytical: $\text{Re}(E_+)$



Maxw. numerical: $\text{Re}(E_+)$



Absorbed fraction	Maxw. analytical	Maxw. numerical
2nd Harmonic D	10.18	9.91
Fundamental H	69.95	70.50
Electrons - FW	11.35	11.21
Electrons - IBW	8.53	8.38

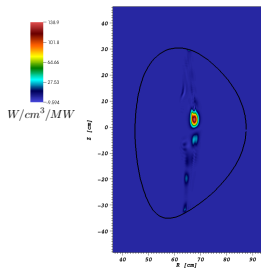
Bi-Maxwellian distribution

$$f_H(v_{\parallel}, v_{\perp}) = (2\pi)^{-3/2} (v_{th,\parallel} v_{th,\perp}^2)^{-1} \exp[-(v_{\parallel}/v_{th,\parallel})^2 - (v_{\perp}/v_{th,\perp})^2]$$

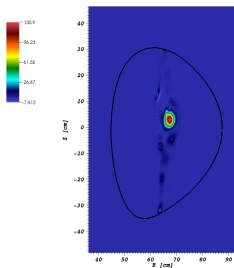
with $v_{th,\parallel} = \sqrt{2C_{\parallel}T(\psi)/m_H}$, $v_{th,\perp} = \sqrt{2C_{\perp}T(\psi)/m_H}$, with constants C_{\parallel} and C_{\perp}

- For $C_{\parallel} = 1$ and $C_{\perp} = \{.5, 1., 3., 5.\}$, P_H , varied by less than 2%
- For $C_{\perp} = 1$ and $C_{\parallel} = \{.5, 1., 3., 5.\}$, the corresponding $P_H = \{61.27\%, 70.50\%, 90.46\%, 94.18\%\}$
 - for small C_{\parallel} , the absorption profile is localized to the resonant layer
 - for large C_{\parallel} , the absorption profile is significantly broadened radially

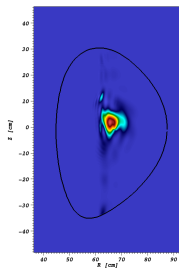
$C_{\perp} = 1, C_{\parallel} = 0.5$



$C_{\perp} = 1, C_{\parallel} = 1$



$C_{\perp} = 1, C_{\parallel} = 5.0$



Non-Maxwellian extension of TORIC v.5 in HHFW heating regime

The susceptibility for a hot plasma with an arbitrary distribution function

Local coordinate frame $(\hat{x}, \hat{y}, \hat{z})$ with $\hat{z} = \hat{b}$ and $\mathbf{k} \cdot \hat{y} = 0$ (Stix)

$$\chi_s = \frac{\omega_{ps}^2}{\omega} \int_0^{+\infty} 2\pi v_{\perp} dv_{\perp} \int_{-\infty}^{+\infty} dv_{\parallel} \hat{\mathbf{z}} \hat{\mathbf{z}} \frac{v_{\parallel}^2}{\omega} \left(\frac{1}{v_{\parallel}} \frac{\partial f}{\partial v_{\parallel}} - \frac{1}{v_{\perp}} \frac{\partial f}{\partial v_{\perp}} \right)_s +$$

$$+ \frac{\omega_{ps}^2}{\omega} \int_0^{+\infty} 2\pi v_{\perp} dv_{\perp} \int_{-\infty}^{+\infty} dv_{\parallel} \sum_{n=-\infty}^{+\infty} \left[\frac{v_{\perp} U}{\omega - k_{\parallel} v_{\parallel} - n\Omega_{cs}} \mathbf{T}_n \right]$$

where

$$U \equiv \frac{\partial f}{\partial v_{\perp}} + \frac{k_{\parallel}}{\omega} \left(v_{\perp} \frac{\partial f}{\partial v_{\parallel}} - v_{\parallel} \frac{\partial f}{\partial v_{\perp}} \right) \quad \text{and}$$

$$\mathbf{T}_n = \begin{pmatrix} \frac{n^2 J_n^2(z)}{z^2} & \frac{inJ_n(z)J'_n(z)}{z} & \frac{nJ_n^2(z)v_{\parallel}}{zv_{\perp}} \\ -\frac{inJ_n(z)J'_n(z)}{z} & (J'_n(z))^2 & -\frac{iJ_n(z)J'_n(z)v_{\parallel}}{v_{\perp}} \\ \frac{nJ_n^2(z)v_{\parallel}}{zv_{\perp}} & \frac{iJ_n(z)J'_n(z)v_{\parallel}}{v_{\perp}} & \frac{J_n^2(z)v_{\parallel}^2}{v_{\perp}^2} \end{pmatrix}, \quad z \equiv \frac{k_{\perp} v_{\perp}}{\Omega_{cs}}$$

Numerical evaluation of χ needed for arbitrary distribution function

- The “best” approach for a complete extension of the code is to implement directly the general expression for χ (previous slide)
 - Plemelj’s formula $\rightarrow \frac{1}{\omega - \omega_0 \pm i0} = \wp \frac{1}{\omega - \omega_0} \mp i\pi\delta(\omega - \omega_0)$
- Integrals in the expression for χ are computed numerous times in TORIC-HHFW so **an efficient evaluation is essential**
- Strong similarity of the generalization done in TORIC-IC regime
 - integrals in the v_{\parallel} -space with the singularity function $(\omega - k_{\parallel}v_{\parallel} - n\Omega_{cs})^{-1}$
 - general integrals’ structure and logic of the implementation
 - for TORIC-HHFW: to reconstruct the new integrands including the sum over the harmonic number n and the k_{\perp} dependence in the argument of the Bessel functions
- Precomputation of χ

The susceptibility for a hot plasma with a Maxwellian distribution function can be evaluated analitically

$$\chi_s = \left[\hat{\mathbf{z}}\hat{\mathbf{z}} \frac{2\omega_p^2}{\omega k_{\parallel} v_{th}^2} \langle v_{\parallel} \rangle + \frac{\omega_p^2}{\omega} \sum_{n=-\infty}^{+\infty} e^{-\lambda} \mathbf{Y}_n(\lambda) \right]_s$$

where

$$\mathbf{Y}_n = \begin{pmatrix} \frac{n^2 I_n}{\lambda} A_n & -in(I_n - I'_n)A_n & \frac{k_{\perp}}{\omega_c} \frac{nI_n}{\lambda} B_n \\ in(I_n - I'_n)A_n & \left(\frac{n^2}{\lambda} I_n + 2\lambda I_n - 2\lambda I'_n \right) A_n & \frac{ik_{\perp}}{\omega_c} (I_n - I'_n)B_n \\ \frac{k_{\perp}}{\omega_c} \frac{nI_n}{\lambda} B_n & -\frac{ik_{\perp}}{\omega_c} (I_n - I'_n)B_n & \frac{2(\omega - n\omega_c)}{k_{\parallel} v_{th}^2} I_n B_n \end{pmatrix}$$

$$A_n = \frac{1}{k_{\parallel} v_{th}} Z_0(\zeta_n), \quad B_n = \frac{1}{k_{\parallel}} (1 + \zeta_n Z_0(\zeta_n)), \quad Z_0(\zeta_n) \equiv \text{plasma dispersion func.}$$

$$\zeta_n \equiv \frac{\omega - n\omega_c}{k_{\parallel} v_{th}}, \quad \lambda \equiv \frac{k_{\perp}^2 v_{th}^2}{2\Omega_c^2}$$

Good agreement between numerical and analytical evaluation of the full hot dielectric tensor

Parameters:

$$f = 30 \times 10^6 \text{ Hz}; n_{\text{dens}} = 5 \times 10^{13} \text{ cm}^{-3},$$

$$N_{\parallel} = 10, B = 0.5 \text{ T}, T_i = 20 \text{ keV}$$

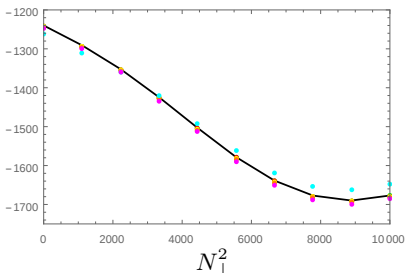
$$N_{\text{harmonics}} = 10$$

Ion species: Deuterium

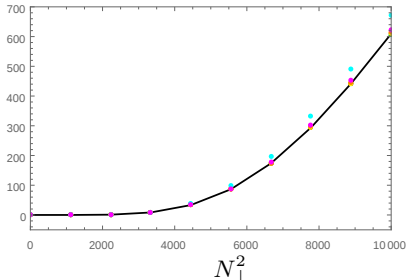
Black curve: analytical solution

	$N_{v_{\parallel}}$	$N_{v_{\perp}}$
●	100	50
●	200	100
●	324	150
●	650	300
●	1300	600
●	2600	1200

$\text{Re}(\epsilon_{xx})$

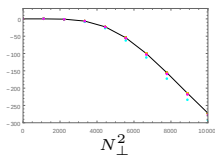


$\text{Im}(\epsilon_{xx})$

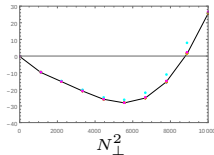


Good agreement between numerical and analytical evaluation of the full hot dielectric tensor (2)

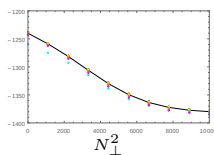
$\text{Re}(\epsilon_{xy})$



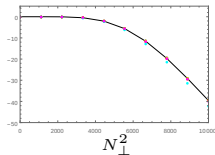
$\text{Re}(\epsilon_{yy})$



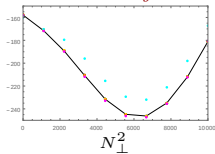
$\text{Re}(\epsilon_{xz})$



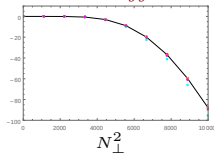
$\text{Re}(\epsilon_{yz})$



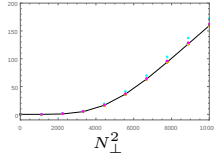
$\text{Im}(\epsilon_{xy})$



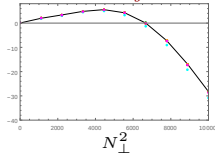
$\text{Im}(\epsilon_{yy})$



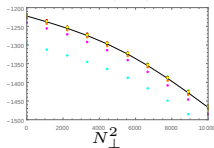
$\text{Im}(\epsilon_{xz})$



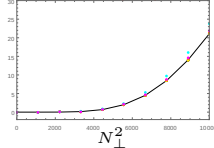
$\text{Im}(\epsilon_{yz})$



$\text{Re}(\epsilon_{zz})$



$\text{Im}(\epsilon_{zz})$

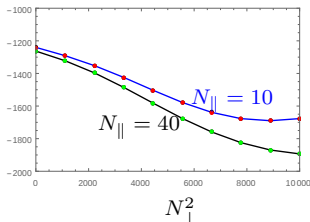


Good agreement between numerical and analytical evaluation of the full hot dielectric tensor: Test on N_{\parallel}

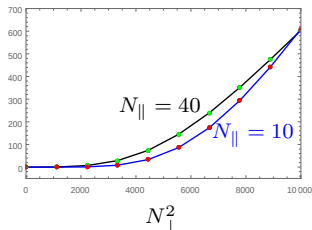
Black and Blue lines:
analytical solutions

	$N_{v_{\parallel}}$	$N_{v_{\perp}}$
● ●	2600	1200

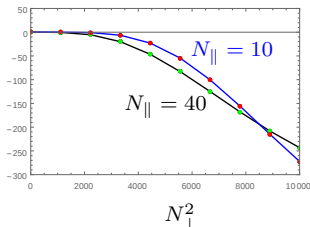
$\text{Re}(\epsilon_{xx})$



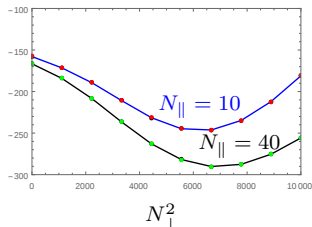
$\text{Im}(\epsilon_{xx})$



$\text{Re}(\epsilon_{xy})$



$\text{Im}(\epsilon_{xy})$

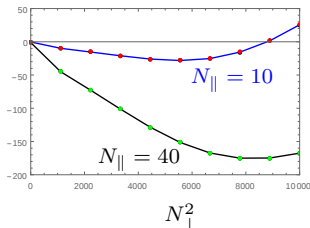


Good agreement between numerical and analytical evaluation of the full hot dielectric tensor: Test on N_{\parallel}

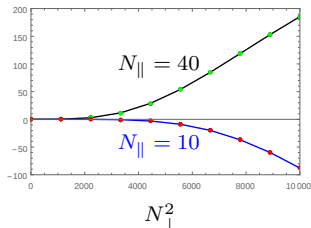
Black and Blue lines:
analytical solutions

	$N_{v_{\parallel}}$	$N_{v_{\perp}}$
● ●	2600	1200

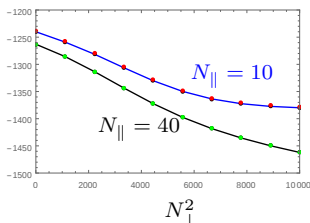
$\text{Re}(\epsilon_{xz})$



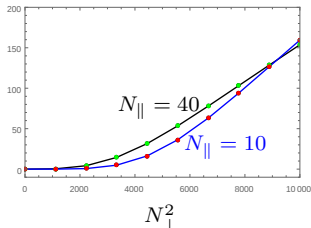
$\text{Im}(\epsilon_{xz})$



$\text{Re}(\epsilon_{yy})$



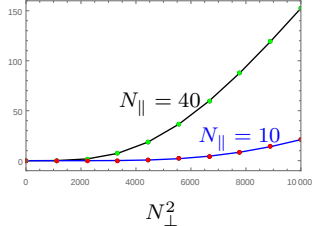
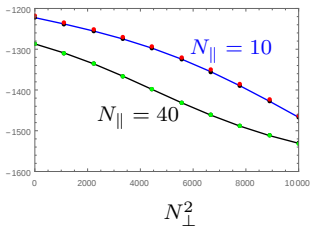
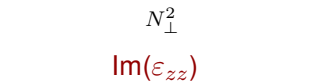
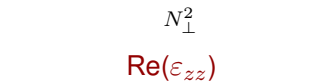
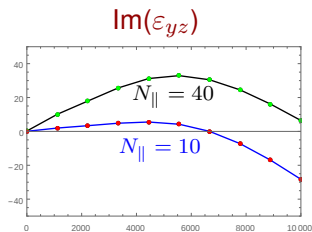
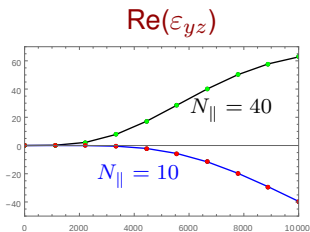
$\text{Im}(\epsilon_{yy})$



Good agreement between numerical and analytical evaluation of the full hot dielectric tensor: Test on N_{\parallel}

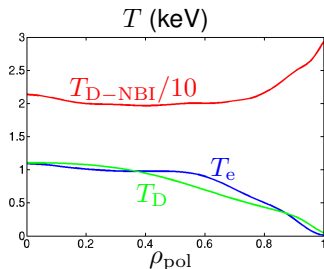
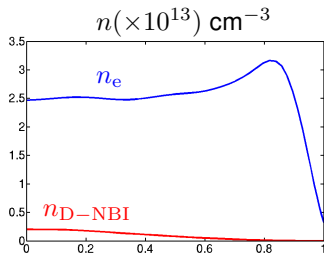
Black and Blue lines:
analytical solutions

	$N_{v_{\parallel}}$	$N_{v_{\perp}}$
● ●	2600	1200



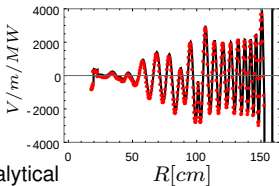
Main parameters:

- Plasma species: electron, D, D-NBI (4%)
- $B_T = 0.529$ T
- $I_p = 868$ kA
- $q(0) = 1.52$
- q at plasma edge = 18.151
- $T_e(0) = 1.093$ keV
- $n_e(0) = 2.467 \times 10^{13}$ cm $^{-3}$
- $T_D(0) = 1.104$ keV
- $T_{D-NBI}(0) = 21.374$ keV
- $n_{D-NBI}(0) = 2.011 \times 10^{12}$ cm $^{-3}$
- TORIC resolution: $n_{mod} = 31$, $n_{elm} = 200$

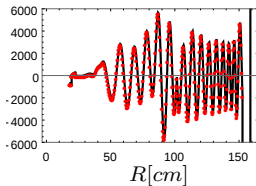


Excellent agreement between numerical and analytical evaluation of HHFW fields in the midplane

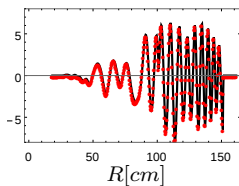
$\text{Re}(E_-)$



$\text{Re}(E_+)$



$\text{Re}(E_{\parallel})$

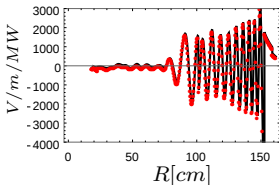


— Analytical

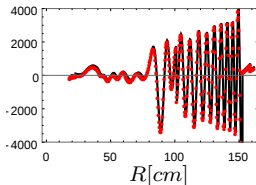
● Numerical

$N_{v_{\parallel}} = 100, N_{v_{\perp}} = 50$

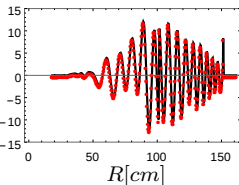
$\text{Im}(E_-)$



$\text{Im}(E_+)$

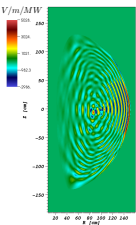


$\text{Im}(E_{\parallel})$

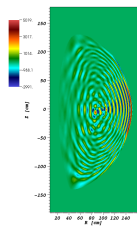


Excellent agreement between numerical and analytical evaluation of the 2D HHFW fields and in terms of absorbed power

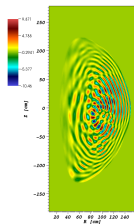
Maxw. analytical: $\text{Re}(E_-)$



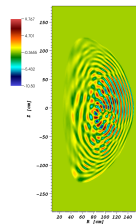
Maxw. numerical: $\text{Re}(E_-)$



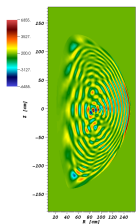
Maxw. analytical: $\text{Re}(E_{||})$



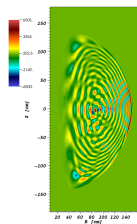
Maxw. numerical: $\text{Re}(E_{||})$



Maxw. analytical: $\text{Re}(E_+)$



Maxw. numerical: $\text{Re}(E_+)$



Absorbed fraction	Maxw. analytical	Maxw. numerical
D	0.22	0.22
D-NBI	73.88	73.58
Electrons	25.90	26.21

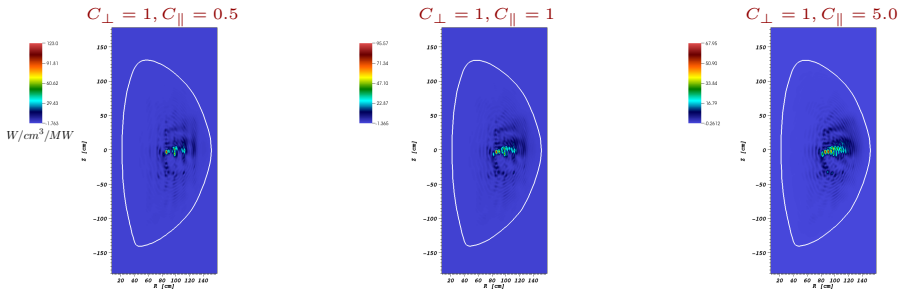
Resolution used for χ : $N_{v_{||}} = 100$ and $N_{v_{\perp}} = 50$

Bi-Maxwellian distribution

$$f_D(v_{\parallel}, v_{\perp}) = (2\pi)^{-3/2} (v_{th,\parallel} v_{th,\perp}^2)^{-1} \exp[-(v_{\parallel}/v_{th,\parallel})^2 - (v_{\perp}/v_{th,\perp})^2]$$

with $v_{th,\parallel} = \sqrt{2C_{\parallel}T(\psi)/m_D}$, $v_{th,\perp} = \sqrt{2C_{\perp}T(\psi)/m_D}$, with constants C_{\parallel} and C_{\perp}

- For $C_{\perp} = 1$ and $C_{\parallel} = \{.5, 1., 3., 5.\}$, P_{D-NBI} , varied by less than 1%
 - Opposite behavior w.r.t. the IC minority heating regime
 - however, for small (large) C_{\parallel} , the absorption profile is localized to the resonant layers (significantly broadened radially), as found in the IC minority heating regime
- For $C_{\parallel} = 1$ and $C_{\perp} = \{.5, 1., 3., 5.\}$, the corresponding $P_{D-NBI} = \{70.06, 73.56, 62.84, 48.48\}$



Slowing-down distribution

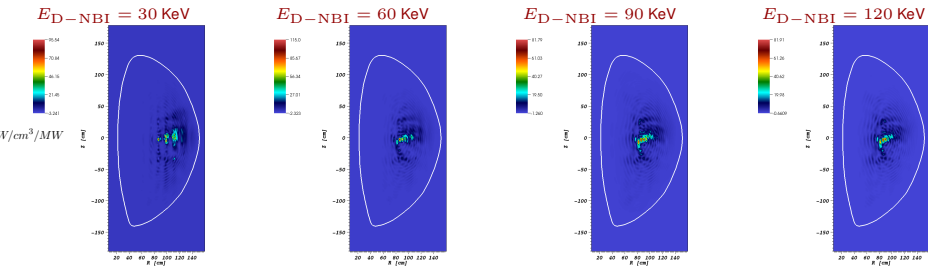
$$f_D(v_{\parallel}, v_{\perp}) = \begin{cases} \frac{A}{v_c^3} \frac{1}{1+(v/v_c)^3} & \text{for } v < v_m, \\ 0 & \text{for } v > v_m \end{cases} \quad v_m \equiv \sqrt{2E_{D-NBI}/m_D}$$

$$A = 3/[4\pi \ln(1 + \delta^{-3})], \quad \delta \equiv \frac{v_c}{v_m}, \quad v_c = 3\sqrt{\pi}(m_e/m_D)Z_{\text{eff}}v_{\text{th}}^3, \quad Z_{\text{eff}} \equiv \sum_{\text{ions}} \frac{Z_i^2 n_i}{A_i n_e}$$

For $Z_{\text{eff}} = 2$ and $E_{D-NBI} = 30, 60, 90, 120$ keV $\Rightarrow P_{D-NBI} = \{77.84\%, 75.85\%, 70.97\%, 64.71\%\}$

- Similar behavior when varied C_{\perp} in the bi-Maxwellian case
- Fast ions absorption, in fact, should decrease with something like $T_{\text{fast ions}}^{-3/2}$

■ This is due to the behavior of the function $f(\lambda) = \lambda I_n e^{-\lambda}$, which reached a maximum value at $\lambda = n^2/3$. For large λ , $f(\lambda) \propto \lambda^{-3/2}$ [See Stix's book & Ono, PoP 1995]



Conclusions

- Non-Maxwellian extension of TORIC in minority heating regime reproduces previous simulations
 - Excellent agreement of the 2D electric field and in terms of absorbed power
- Implementation of the full hot dielectric tensor reproduces the analytic Maxwellian case
- Non-Maxwellian extension of TORIC in HHFW regime reproduces previous simulations
 - Excellent agreement of the 2D electric field and in terms of absorbed power
- For bi-Maxwellian distribution found two different behaviors:
 - for IC minority heating regime, the absorbed power at the H fundamental is insensitive to variations in T_{\perp} , but varies with changes in T_{\parallel}
 - for HHFW heating regime, the fast ions absorbed power is insensitive to variations in T_{\parallel} , but varies with changes in T_{\perp}
 - however, absorption profile varies with changes in T_{\parallel}
- For slowing down distribution in the HHFW heating regime, the fast ions absorbed power varies with changes in E_{NBI}
 - $P_{\text{D-NBI}}$ decreases with increasing E_{NBI}
 - similar behavior found at large T_{\perp} in the bi-Maxwellian case